

## Original Article

**Running Title:** TILs and MRI in HCC

Received: January 1, 2026; Accepted: May 24, 2026

### **Impact of MRI Findings and Clinical Parameters on Predicting Tumor-Infiltrating Lymphocytes in Hepatocellular Carcinoma Patients**

Yaser Arafat\*, MD, Amrallah Mohammed\*†, PhD, Ahmad BarakatWaley\*, MD, Basma K Soliman\*\*, MD, Mohamed S. Bayomi\*\*\*, MD, Amira Hanna\*\*\*\*, MD, Basant EL-Shafaay\*\*\*\*, MD, Marwa M. EL- Mosely\*\*\*\*, MD, Doaa Mandour\*\*\*\*, MD

\**Medical Oncology Department, Faculty of Medicine, Zagazig University, Egypt*

\*\**Radiodiagnosis Department, Faculty of Medicine, Zagazig University, Egypt*

\*\*\**General Surgery Department, Faculty of Medicine, Zagazig University, Egypt*

\*\*\*\**Clinical Oncology and Nuclear Medicine Department, Faculty of Medicine, Zagazig University, Egypt*

\*\*\*\*\**Pathology Department, Faculty of Medicine, Zagazig University, Egypt*

#### **♦Corresponding Author**

Amrallah Mohammed, MD

Medical Oncology Department,

Faculty of Medicine,

Zagazig University, Egypt

Email: [amrallaabdelmoneem@yahoo.com](mailto:amrallaabdelmoneem@yahoo.com)

#### **Abstract**

**Background:** The preoperative identification of tumor-infiltrating lymphocyte (TIL) status in hepatocellular carcinoma (HCC) is clinically important, but the ability of magnetic resonance imaging (MRI) features combined with clinical parameters to predict TIL levels remains unclear. The present study aimed to investigate whether MRI features and clinical parameters can predict TIL levels in patients with HCC undergoing surgical resection.

**Method:** A retrospective study of 156 HCC patients categorized TILs into; group 0 (low TIL, 0%–10%), group 1 (intermediate TIL, 11%–59%), and group 2 (high TIL, ≥60%). Continuous and categorical variables were compared using appropriate tests. Logistic regression identified predictors of TILs.

**Results:** Of 131 included patients, 37.9% were included in group 0, 12.2% in group 1, and 50.4% in group 2. Group 0 was significantly associated with ≥60 years of age, grade III, microvascular invasion, alpha-fetoprotein (AFP) >400 ng/ml, satellite nodules, unclear tumor boundaries, irregular shapes, non-smooth margins, absence of tumor capsule, and larger size ( $P < 0.05$  for all). AFP level (odds ratio (OR) 0.19; 95% confidence interval (CI) 0.08-0.75,  $P = 0.03$ ), tumor shape (OR 6.31; 95% CI 2.44-40.31,  $P = 0.01$ ), margin (OR 0.13; 95% CI 0.05-0.6,  $P = 0.03$ ), and tumor size on MRI (OR 0.99; 95% CI 1.06-1.49,  $P = 0.04$ ) were independent predictors of TIL levels.

**Conclusion:** Preoperative MRI features, including tumor morphology, margin characteristics, and tumor size, together with serum AFP levels, showed a significant value in predicting TIL density in HCC patients undergoing surgical resection. These findings highlight MRI as a non-invasive tool for preoperative assessment and risk stratification.

**Keywords:** Hepatocellular carcinoma, Tumor-infiltrating lymphocytes, Magnetic resonance imaging

## **Introduction**

Hepatocellular carcinoma (HCC) is a very aggressive form of liver malignancy that typically arises in people with cirrhosis or chronic liver disease. Its global incidence is steadily increasing and is expected to continue rising through 2030. The high prevalence of hepatitis either B and/ or C infections in Africa and Asia contributes substantially to the burden of HCC, as these infections promote chronic liver affection with subsequent malignant transformation.<sup>1</sup> Despite the availability of screening programs, a significant number of HCC cases are detected at advanced stages, which is associated with poor survival outcomes.<sup>2</sup> Treatment options that can cure the condition are restricted for patients who are not eligible for surgical resection or orthotopic liver transplantation.<sup>3</sup> Even among patients who undergo resection, recurrence remains a major challenge, with up to 75% experiencing the development of new HCC lesions or local recurrence within five years.<sup>4</sup> Several clinical and pathological factors have been shown to influence HCC prognosis, including elevated alpha-fetoprotein (AFP), tumor histological grade, the extent of liver fibrosis, and tumor-infiltrating lymphocytes (TILs).<sup>5,6</sup> TILs are immune cells present both within the tumor mass and in the surrounding tissue, and their presence has been linked to improved survival outcomes across numerous cancer types.<sup>7</sup> HCC can often be diagnosed without tissue sampling when nodules of 1 cm or larger exhibit the characteristic imaging pattern of arterial phase hyper enhancement followed by venous phase washout on computed tomography (CT) or magnetic resonance imaging (MRI).<sup>8</sup> MRI has been shown to outperform CT in detecting small HCC

lesions, providing a more precise evaluation of tumor characteristics.<sup>9</sup>

Although MRI is well-established as a diagnostic tool for HCC, its potential to provide prognostic information, particularly in predicting immune cell infiltration, has not been fully explored. Therefore, the present study aimed to investigate the relationship between MRI features, clinical parameters, and TIL levels in patients with HCC undergoing surgical resection.

## **Patients and Methods**

### ***Ethical approval***

We obtained clearance for this retrospective analysis from the Institutional Review Board (IRB) of Zagazig University Hospital (ethics code: ZU-IRB#497 /11). Due to the retrospective design of the study, the requirement for informed consent was waived.

### ***Study design and patient selection***

This retrospective analysis included patients with HCC who were diagnosed and treated at the Departments of Medical Oncology, Pathology, Radiology, and Surgery, Faculty of Medicine, Zagazig University, between January 2017 and December 2022. Clinical and radiological data were obtained through chart review and the hospital's Picture Archiving and Communication System (PACS).

The inclusion criteria were: age  $\geq 18$  years, resectable, operable, and MRI findings consistent with HCC obtained within two weeks prior to surgery. Patients were excluded if they had received any preoperative systemic or local therapy directed to the tumors, or if clinical, pathological, or radiological data were incomplete. For patients with multifocal tumors, the lesion with the largest diameter

was selected for analysis. A flow diagram of patient selection is presented in Figure 1.

### **Data collection**

#### **Clinical and pathological parameters**

Collected clinical data included age, sex, liver function tests, AFP levels, and hepatitis virus status. Pathological variables included tumor size, histologic grade, and the presence of microvascular invasion (MVI).

#### **MRI features**

MRI was reviewed by our radiodiagnosis consultant. MRI assessment concentrated on multiple morphologic and structural tumor features, including necrotic components, the presence of satellite lesions, capsular appearance, lesion boundary definition, margin characteristics, overall tumor configuration, and the largest tumor dimension. The examinations were performed on 1.5 T and 3.0 T clinical scanners. A standardized liver MRI protocol included axial T1-weighted GRE, axial T2-weighted FSE with and without fat suppression, and diffusion-weighted imaging (b-values 0–800 s/mm<sup>2</sup>). Dynamic contrast-enhanced imaging was performed following intravenous administration of a gadolinium-based contrast agent (0.1 mmol/kg at 2–3 mL/s with saline flush). Three dynamic phases were acquired: arterial (~20 s), portal venous (~60–70 s), and late venous (~3–4 min) post-injection, with sequence parameters optimized for high spatial resolution. Additional hepatobiliary phase imaging at 20 min was included when hepatocyte-specific contrast agents were used. This protocol allowed a comprehensive evaluation of lesion morphology, enhancement patterns, and ancillary features. Necrosis was identified as intratumoral areas lacking post-contrast enhancement and exhibiting high signal intensity on T2-weighted sequences. Satellite nodules were defined as discrete lesions detected within a 2-cm radius of the primary tumor. Capsular formation was recognized by the appearance

of a hyperintense peripheral rim during the venous or equilibrium contrast phases. Lesion boundaries were evaluated as either clearly demarcated or indistinct, while tumor margins were classified as smooth or irregular. Tumor morphology was categorized as round or non-round, and tumor size was determined by measuring the greatest transverse diameter on axial MRI images (Figure 2).

#### **Histopathological assessment**

The resected specimens were reviewed by our pathologist. The specimens were fixed in paraffin, and immunohistochemistry was performed to evaluate TILs. TIL density and percentage were calculated according to International Working Group criteria:<sup>10</sup>

- **Group 0:** low infiltration (0%–10%)
- **Group 1:** moderate infiltration (11%–59%)
- **Group 2:** high infiltration ( $\geq 60\%$ )

Representative immunohistochemistry images illustrating each group are provided in Figure 3.

#### **Statistical analysis**

The study used the Mann-Whitney U test, independent samples t-test, and chi-squared test to analyze continuous and categorical variables. Univariate and multivariate logistic regression analyses were conducted to examine the clinical variables and MRI parameters associated with TILs. Continuous variables were presented as mean  $\pm$  standard deviation or median (interquartile range) values and compared using independent-samples t-tests or the Mann-Whitney U test. Categorical variables were presented as numbers (percentages) and compared using the chi-square test. Univariate analysis was conducted to identify potentially significant variables. Variables with significant differences ( $P < 0.05$ ) in the univariate analysis were included in multivariate analysis to identify independent predictors of TILs. Statistical analyses were carried out using SPSS 22.0 for Windows (IBM, Inc.,

Chicago, IL, USA) and MedCalc for Windows (MedCalc Software bvba, Ostend, Belgium).

## Results

Out of 156 initially identified patients, 25 were excluded due to incomplete MRI data, leaving 131 eligible patients. The cohort included 94 men, with a mean age of  $61.3 \pm 8.7$  years. Tumor distribution among TIL groups was: 49 patients (37.9%) in group 0, 16 (12.2%) in group 1, and 66 (50.4%) in group 2. Fourteen patients had multifocal tumors; in these cases, the largest lesion was analyzed. Table 1 provides a summary of the key clinical and pathological features.

### *Associations between TILs and clinical/MRI features*

Group 0 (TILs 0%–10%) was associated with several unfavorable features, including age  $\geq 60$  years, grade III tumors, presence of MVI, AFP  $> 400$  ng/mL, presence of satellite nodules, unclear tumor boundary, irregular (non-rounded) tumor shape, non-smooth tumor margin, absence of a tumor capsule, and larger tumor size ( $P < 0.05$  for all) (Table 2).

### *Independent predictors of TILs*

Logistic regression analysis identified AFP level (odds ratio (OR) 0.19; 95% confidence interval (CI) 0.08–0.75;  $P = 0.03$ ), tumor shape (OR 6.31; 95% CI 2.44–40.31;  $P = 0.01$ ), tumor margin (OR 0.13; 95% CI 0.05–0.60;  $P = 0.03$ ), and tumor size on MRI (OR 0.99; 95% CI 1.06–1.49;  $P = 0.04$ ) as statistically significant independent predictors of TILs (Table 3).

## Discussion

The present study investigated how clinical data and MRI characteristics can help estimate the level of TILs in HCC patients undergoing resection. We found that tumors with low TIL density (0%–10%) were consistently associated with more aggressive histopathological, laboratory, and imaging

characteristics. Notably, serum AFP level and MRI features including tumor size, morphology, and margin features emerged as independent determinants of TILs density.

HCC displays substantial immune involvement, as the tumor microenvironment contains a wide array of interacting inflammatory and immune cell populations.<sup>11</sup> Immune activity can both impede and support tumor development on one hand, eliminating malignant cells, and on the other enabling survival of more resistant clones or fostering conditions that permit tumor expansion. The prognostic effect of TILs may reflect their ability to counterbalance immunosuppressive components within the tumor milieu.<sup>12</sup>

Prior research has established the relevance of TILs across several cancer types, where their presence has been linked to treatment response and overall outcome.<sup>13–17</sup> A meta-analysis by Gooden et al. highlighted the prognostic value of TILs in a range of solid tumors, including HCC.<sup>18</sup> Similarly, the work of Gao et al. demonstrated that higher TIL levels correlate with improved survival in resectable HCC,<sup>19</sup> and findings from a larger pooled analysis also supported this association.<sup>20</sup>

In our cohort, several MRI features differed notably between patients with high and low TIL infiltration. Tumor contour, boundary definition, presence of a capsule, and lesion shape showed clear variation. Tumor shape, margin, and size retained independent predictive value even after adjustment for other variables. These observations partially parallel the results of Du et al., who also reported that lower TIL levels were associated with larger tumors, absence of a capsule, and inferior survival outcomes.<sup>5</sup>

MVI remains a pivotal factor in recurrence and metastatic potential. Patients with greater lymphocytic infiltration appear to develop MVI less frequently, although the

mechanisms underlying this trend require additional clarification.<sup>21</sup>

While multiple studies support the prognostic role of TILs, imaging-based assessment of immune infiltration remains an emerging field. Prior work, including studies by Liao et al. and Chen et al., suggests that radiologic features and radiomic signatures may reflect the degree of lymphocytic infiltration.<sup>22-23</sup> The ability of contrast-enhanced MRI to characterize tumor structure, vascular behavior, and tissue composition makes it well suited for such evaluations.<sup>24</sup>

Integrating clinical variables with imaging findings and pathological information can help refine individualized treatment strategies and may guide decisions regarding surgical management and systemic or immunotherapeutic interventions.

This study is subject to certain limitations, including its retrospective design, relatively small sample size, and single-center setting, which may limit the generalizability of the findings. In patients with multifocal disease, only the largest lesion was evaluated, potentially underrepresenting intratumoral and intertumoral heterogeneity. Furthermore, variability in MRI acquisition parameters and scanner platforms may have introduced imaging protocol heterogeneity, which could have influenced image interpretation and quantitative analysis.

### **Conclusion**

Low TIL density (0–10%) was associated with several adverse features, including older age ( $\geq 60$  years), higher tumor grade, MVI, AFP  $> 400$  ng/mL, and MRI findings such as satellite nodules, irregular tumor contours, non-smooth margins, loss of capsule integrity, and larger tumor size. AFP level, tumor shape, tumor margin, and MRI-based tumor size were identified as independent predictors of TIL levels. These results highlight the potential role of TIL assessment in treatment planning and support the need

for larger prospective studies to determine how immune infiltration may influence the selection of adjuvant or neoadjuvant therapies.

### **Data Availability Statement**

The data supporting the findings of this study are available from the corresponding author upon reasonable request and the IRB approval.

### **Acknowledgements**

I would like to thank the entire medical oncology team for their assistance.

### **Authors' Contribution**

Amrallah Mohammed, Yaser Arafat, Ahmad Barakat Waley, Basma Soliman, Amira Hanna, Marwa EL- Mosely, Mohamed Bayomi, Basant SH, and Doaa Mandour: idea, data collection, interpretation, and discussion.

All authors contributed to study design, data collection and analysis, drafted and revised the manuscript, and approved the final version

### **Funding**

Not applicable.

### **Conflict of Interest**

None declared.

### **References**

1. Singh SP, Madke T, Chand P. Global epidemiology of hepatocellular carcinoma. *J Clin Exp Hepatol.* 2025;15(2):102446. doi:10.1016/j.jceh.2024.102446. PMID: 39659901; PMCID: PMC11626783.
2. Parra NS, Ross HM, Khan A, Wu M, Goldberg R, Shah L, et al. Advancements in the diagnosis of hepatocellular carcinoma. *Int J Transl Med.* 2023;3:51-65. doi:10.3390/ijtm3010005.

3. Cucchetti A, Elshaarawy O, Han G, Chong CCN, Serra C, O'Rourke JM, et al. 'Potentially curative therapies' for hepatocellular carcinoma: how many patients can actually be cured? *Br J Cancer*. 2023;128(9):1665-71. doi: 10.1038/s41416-023-02188-z. PMID: 36807338; PMCID: PMC10133312.
4. Cucchetti A, Zhong J, Berhane S, Toyoda H, Shi K, Tada T, et al. The chances of hepatic resection curing hepatocellular carcinoma. *J Hepatol*. 2020;72(4):711-7. doi: 10.1016/j.jhep.2019.11.016. PMID: 31790765.
5. Du M, Cai YM, Yin YL, Xiao L, Ji Y. Evaluating tumor-infiltrating lymphocytes in hepatocellular carcinoma using hematoxylin and eosin-stained tumor sections. *World J Clin Cases*. 2022;10(3):856-69. doi: 10.12998/wjcc.v10.i3.856. PMID: 35127901; PMCID: PMC8790462.
6. Chen YD, Zhang L, Zhou ZP, Lin B, Jiang ZJ, Tang C, et al. Radiomics and nomogram of magnetic resonance imaging for preoperative prediction of microvascular invasion in small hepatocellular carcinoma. *World J Gastroenterol*. 2022;28(31):4399-416. doi: 10.3748/wjg.v28.i31.4399. PMID: 36159011; PMCID: PMC9453772.
7. Dakal TC, George N, Xu C, Suravajhala P, Kumar A. Predictive and prognostic relevance of tumor-infiltrating immune cells: Tailoring personalized treatments against different cancer types. *Cancers (Basel)*. 2024;16(9):1626. doi: 10.3390/cancers16091626. PMID: 38730579; PMCID: PMC11082991.
8. Hectors SJ, Wagner M, Bane O, Besa C, Lewis S, Remark R, et al. Quantification of hepatocellular carcinoma heterogeneity with multiparametric magnetic resonance imaging. *Sci Rep*. 2017;7(1):2452. doi: 10.1038/s41598-017-02706-z. PMID: 28550313; PMCID: PMC5446396.
9. Kovac JD, Milovanovic T, Dugalic V, Dumic I. Pearls and pitfalls in magnetic resonance imaging of hepatocellular carcinoma. *World J Gastroenterol*. 2020;26(17):2012-29. doi: 10.3748/wjg.v26.i17.2012. PMID: 32536771; PMCID: PMC7267693.
10. Mohammed AA, MostafaElsayed F, Algazar M, Rashed HE. Predictive and prognostic value of tumor-infiltrating lymphocytes for pathological response to neoadjuvant chemotherapy in triple negative breast cancer. *Gulf J Oncolog*. 2022;1(38):53-60. PMID: 35156645.
11. Fu Y, Liu S, Zeng S, Shen H. From bench to bed: the tumor immune microenvironment and current immunotherapeutic strategies for hepatocellular carcinoma. *J Exp Clin Cancer Res*. 2019;38(1):396. doi: 10.1186/s13046-019-1396-4. PMID: 31500650; PMCID: PMC6734524.
12. Oura K, Morishita A, Tani J, Masaki T. Tumor immune microenvironment and immunosuppressive therapy in hepatocellular carcinoma: A review. *Int J Mol Sci*. 2021;22(11):5801. doi: 10.3390/ijms22115801. PMID: 34071550; PMCID: PMC8198390.
13. Zheng X, Jin W, Wang S, Ding H. Progression on the roles and mechanisms of tumor-infiltrating t lymphocytes in patients with hepatocellular carcinoma. *Front Immunol*. 2021;12:729705. doi: 10.3389/fimmu.2021.729705. PMID: 34566989; PMCID: PMC8462294.

14. Zhao Y, Deng J, Rao S, Guo S, Shen J, Du F, et al. Tumor infiltrating lymphocyte (TIL) therapy for solid tumor treatment: Progressions and challenges. *Cancers (Basel)*. 2022;14(17):4160. doi: 10.3390/cancers14174160. PMID: 36077696; PMCID: PMC9455018.
15. Dushyanthen S, Beavis PA, Savas P, Teo ZL, Zhou C, Mansour M, et al. Relevance of tumor-infiltrating lymphocytes in breast cancer. *BMC Med*. 2015;13:202. doi: 10.1186/s12916-015-0431-3. PMID: 26300242; PMCID: PMC4547422.
16. Kang BW, Seo AN, Yoon S, Bae HI, Jeon SW, Kwon OK, et al. Prognostic value of tumor-infiltrating lymphocytes in Epstein-Barr virus-associated gastric cancer. *Ann Oncol*. 2016;27(3):494-501. doi: 10.1093/annonc/mdv610. PMID: 26673353.
17. Schalper KA, Brown J, Carvajal-Hausdorf D, McLaughlin J, Velcheti V, Syrigos KN, et al. Objective measurement and clinical significance of TILs in non-small cell lung cancer. *J Natl Cancer Inst*. 2015;107(3):dju435. doi: 10.1093/jnci/dju435. PMID: 25650315; PMCID: PMC4565530.
18. Brummel K, Eerkens AL, de Bruyn M, Nijman HW. Tumour-infiltrating lymphocytes: from prognosis to treatment selection. *Br J Cancer*. 2023;128(3):451-8. doi: 10.1038/s41416-022-02119-4. PMID: 36564565; PMCID: PMC9938191.
19. Gao F, Xie K, Xiang Q, Qin Y, Chen P, Wan H, et al. The density of tumor-infiltrating lymphocytes and prognosis in resectable hepatocellular carcinoma: a two-phase study. *Aging (Albany NY)*. 2021;13(7):9665-78. doi: 10.18632/aging.202710. PMID: 33744864; PMCID: PMC8064144.
20. Yao W, He JC, Yang Y, Wang JM, Qian YW, Yang T, et al. The prognostic value of tumor-infiltrating lymphocytes in hepatocellular carcinoma: a systematic review and meta-analysis. *Sci Rep*. 2017;7(1):7525. doi: 10.1038/s41598-017-08128-1. PMID: 28790445; PMCID: PMC5548736.
21. Torbenson MS, Ng IOL, Park, YN, Roncalli M, Sakamoto M. WHO Classification of Tumours: Digestive System Tumours. 5<sup>th</sup>ed. International Agency for Research on Cancer: Lyon, France, 2019.p.229-239.
22. Liao H, Zhang Z, Chen J, Liao M, Xu L, Wu Z, et al. Preoperative radiomic approach to evaluate tumor-infiltrating CD8+ T cells in hepatocellular carcinoma patients using contrast-enhanced computed tomography. *Ann Surg Oncol*. 2019;26(13):4537-47. doi: 10.1245/s10434-019-07815-9. PMID: 31520208.
23. Chen S, Feng S, Wei J, Liu F, Li B, Li X, et al. Pretreatment prediction of immunoscore in hepatocellular cancer: a radiomics-based clinical model based on Gd-EOB-DTPA-enhanced MRI imaging. *Eur Radiol*. 2019;29(8):4177-87. doi: 10.1007/s00330-018-5986-x. PMID: 30666445.
24. Ronot M, Chernyak V, Burgoyne A, Chang J, Jiang H, Bashir M, et al. Imaging to predict prognosis in hepatocellular carcinoma: Current and future perspectives. *Radiology*. 2023;307(3):e221429. doi: 10.1148/radiol.221429. PMID: 37014244.



Table 2. The distribution of TILs among hepatocellular carcinoma patients included in the study (n = 131)

Features	TILs			P-value
	Group 0 N=49 (%)	Group 1 N=16 (%)	Group 2 N=66 (%)	
<b>Age</b>				
<60 years	15 (20.5)	13 (17.8)	45 (61.7)	0.03
≥ 60 years	34 (58.6)	3 (5.2)	21 (36.2)	
<b>Sex</b>				
Male	25 (26.6)	11 (11.7)	58 (61.7)	0.61
Female	24 (64.9)	5 (13.5)	8 (21.6)	
<b>Grade</b>				
I	4 (20)	5 (25)	11 (55)	0.04
II	14 (25.9)	2 (3.7)	38 (70.4)	
III	31 (54.4)	9 (15.8)	17 (29.8)	
<b>MVI</b>				
Present	33 (52.4)	4 (12.1)	26 (35.5)	0.01
Absent	16 (23.6)	12 (17.6)	40 (48.8)	
<b>Necrosis</b>				
Present	33 (47.1)	8 (11.4)	29 (41.5)	0.82
Absent	16	8	37	
<b>HCV</b>	47 (39.5)	12 (10.1)	60 (50.4)	0.07
<b>Non-HCV</b>	2 (16.7)	4 (33.3)	6 (50)	
<b>Previous anti-virus therapy</b>				
Yes	42 (40.8)	8 (7.8)	51 (51.4)	0.12
No	5 (17.9)	8 (28.6)	15 (53.5)	
<b>AFP (ng/mL)</b>				
<400	6 (10.3)	9 (15.5)	43 (74.2)	<0.001
≥400	43 (58.9)	7 (9.6)	23 (31.5)	
<b>Satellite nodules</b>				
Present	19 (63.3)	5 (16.7)	6 (20)	<0.00
Absent	30 (29.7)	11 (10.9)	60 (59.4)	
<b>Tumor boundary</b>				
Clear	37 (34.9)	10 (9.4)	59 (55.7)	0.02
Unclear	12 (48)	6 (24)	7 (28)	
<b>Tumor shape</b>				
Rounded	22 (25.9)	11 (12.9)	52 (61.2)	0.04
Unrounded	27 (58.7)	5 (10.9)	14 (30.4)	
<b>Tumor margin</b>				
Smooth	22 (27.8)	9 (11.4)	48 (60.8)	<0.001
Non-smooth	27 (51.9)	7 (13.5)	18 (34.6)	
<b>Tumor capsule</b>				
Present	28 (28.6)	12 (12.9)	53 (58.5)	<0.001
Absent	21 (55.3)	4 (10.5)	13 (34.2)	
<b>Tumor size by MRI</b>				
T1	5 (14.7)	11 (32.4)	18 (52.9)	0.01
T2	27 (49.1)	3 (5.5)	25 (45.4)	
T3	17 (40.5)	2 (4.8)	23 (54.7)	
<b>Tumor size on pathology</b>				
T1	2 (11.8)	5 (29.4)	10 (58.8)	0.03
T2	9 (13.8)	5 (7.7)	51 (78.5)	
T3	38 (77.6)	6 (12.2)	5 (10.2)	

Non-rounded morphology was defined as a lobulated or irregular but still well-demarcated expansile mass; AFP: Alpha-fetoprotein; MRI: Magnetic resonance imaging; MVI: Microvascular invasion; HCV: Hepatitis C virus; TILs: Tumor infiltrating lymphocytes; n: Number; P- value<0.05 is considered a significant; Group 0 = low TILs (0%-10%); Group 1= (11%-59%); Group 2 (≥ 60%)

Table 3. Cox proportional hazards regression analyses (univariate and multivariate) for the prediction of TILs in hepatocellular carcinoma patients

Features	Univariate		Multivariate	
	OR (95%CI)	P-value	OR (95%CI)	P-value
Age	0.99 (0.96-1.00)	0.07	--	--
Sex	2.31 (0.96-5.70)	0.91	--	--
Grade	1.12(0.45-2.76)	0.42	--	--
Necrosis	1.90 (0.86-4.20)	0.13	--	--
HCV vs non-HCV	0.58(0.18-1.81)	0.42	--	--
Previous antiviral therapy	1.53 (0.67-3.51)	0.71	--	--
AFP (ng/ml)	0.13 (0.06-0.50)	0.01	0.19 (0.08-0.75)	0.03
Satellite nodules	4.91 (0.93-17.32)	0.03	--	--
Tumor boundary	0.34 (0.09-0.98)	0.14	0.27 (0.09-0.57)	0.42
Tumor shape	8.46 (3.54-22.71)	<0.001	6.31 (2.44-40.31)	0.01
Tumor margin	0.15 (0.06-0.67)	0.002	0.13 (0.05-0.6)	0.03
Tumor capsule	0.56 (0.16-1.98)	0.02	--	--
Tumor size by MRI	1.54 (2.06-2.21)	0.001	0.99 (1.06-1.49)	0.04

AFP: Alpha-fetoprotein; MRI: Magnetic resonance imaging; MVI: Microvascular invasion; HCV: Hepatitis C virus; TILs: Tumor infiltrating lymphocytes; OR: Odds ratio; CI: Confidence interval; P- value<0.05 is considered a significant.

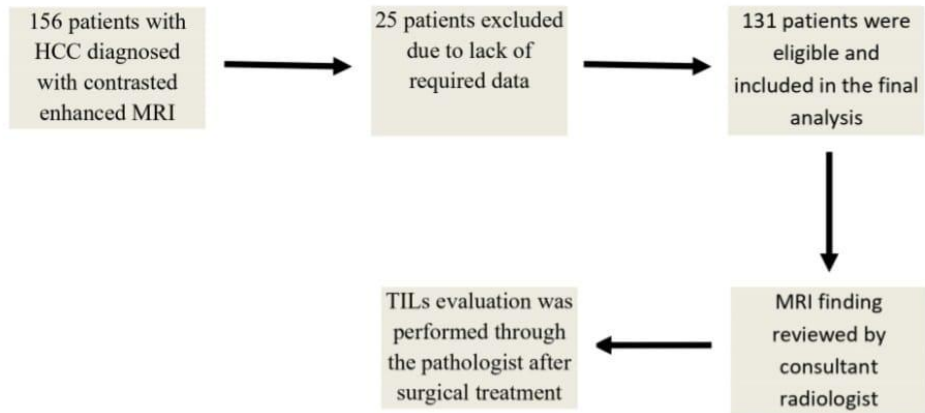


Figure 1. This figure illustrates the flow chart of patient selection and inclusion in the study. It shows the total number of patients initially assessed for eligibility, the number of patients excluded with reasons for exclusion, and the final number of HCC patients included in the analysis.

TILs: Tumor infiltrating lymphocytes; MRI: Magnetic resonance imaging; HCC: Hepatocellular carcinoma



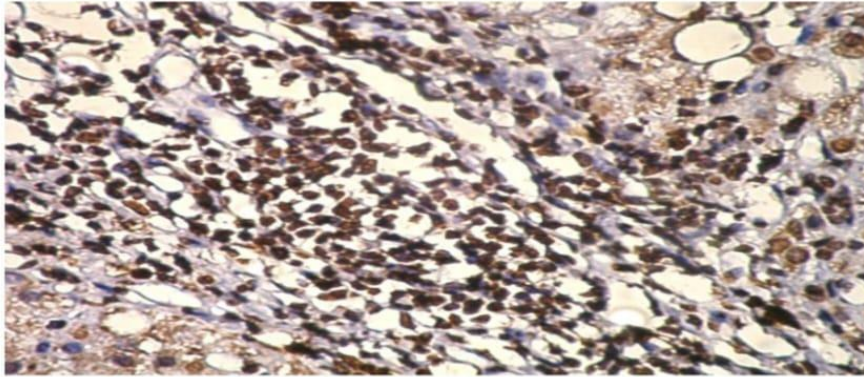


Figure3A

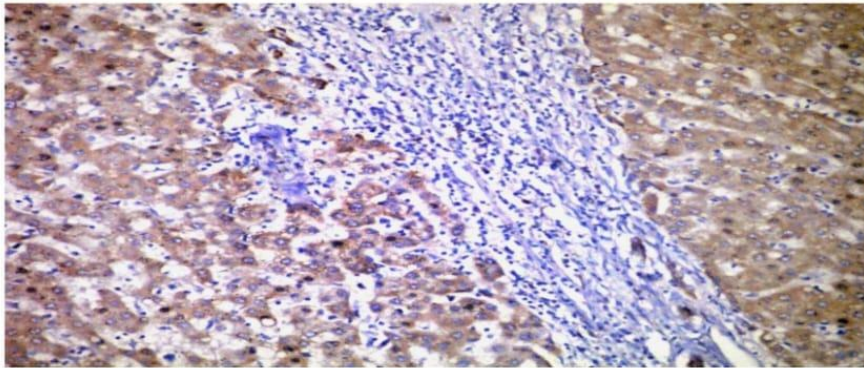


Figure3B

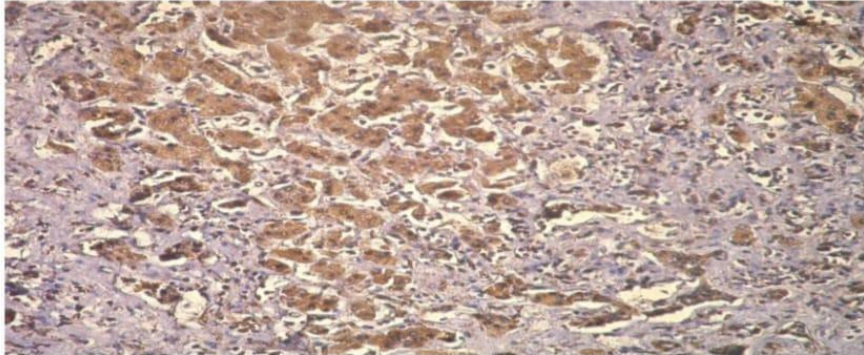


Figure3C

Figure 3. This figure shows hematoxylin and eosin (H&E) staining of TILs in hepatocellular carcinoma tissue sections at  $\times 400$  magnification, Figure 3A demonstrates a tumor with high TILs infiltration ( $\geq 60\%$ ), Figure 3B shows moderate TILs infiltration (11%–59%), and Figure 3C illustrates low TILs infiltration (0%–10%).

TILs: Tumor-infiltrating lymphocytes